Desalination and Water Treatment
www.deswater.com

doi:10.5004/dwt.2019.24605

166 (2019) 158–167
October

Heterogeneous oxidation of sulfacetamide in aquatic environment using ultrasonic and nano-Fenton: kinetics intermediates and bioassay test

Torkan Abdili[a], Ayat Rahmani[b], Hasan Rahmani[c,d], Morteza Alighadri[a], Kourosh Rahmani[e,*]

[a]*Department of Environmental Health Engineering, School of Health, Ardabil University of Medical Sciences, Ardabil, Iran, Tel. +98 45335113775, email: torkan.abdili@yahoo.com (T. Abdili), Tel. +98 33523890, email: m.alighadri@arums.ac.ir (M. Alighadri)*
[b]*Research Center for Health Sciences and Technologies, Semnan University of Medical Sciences, Semnan, Iran, Tel. +98 9333900151, email: ayat_rahmani@yahoo.com (A. Rahmani)*
[c]*Department of Environmental Health Engineering, School of Health, Kashan University of Medical Sciences, Kashan, Iran, Tel. +98 9176146624, email: hs.rahmani@yahoo.com (H. Rahmani)*
[d]*Research Center for Social Determination of Health(SDOH), Kashan University of Medical Sciences, Kashan, Iran, Semnan, Iran,*
[e]*Department of Environmental Health Engineering, Mamasani Higher Education Complex for Health, Shiraz University of Medical Sciences, Shiraz, Iran, Tel. +98 7142541387, Fax +98 7142541387, email: krahmanii@yahoo.com (K. Rahmani)*

Received 27 February 2019; Accepted 22 June 2019

ABSTRACT

In present study, degradation of sulfacetamide from a synthetic wastewater by sonofenton process using zero valent iron nanoparticles was investigated. The synthesized iron nanoparticles were characterized using transmission electron microscopy (TEM), UV-visible and X-ray diffraction pattern (XRD). The effect of various parameters, such as pH, nZVI dose, H_2O_2 concentration and contact time was studied with batch experiments. The removal efficiency of sulfacetamide by US/nZVI/H_2O_f process was about 91% for reaction time of 60 min, but less than 27% of chemical oxygen demand (COD) was removed. Kinetics studies showed that the degradation of sulfacetamide fitted well to the pseudo-second-order model. Using the LC/MS device, five intermediate from degradation of sulfacetamide were detected. The toxicity test, using micro toxicity study also showed that the effluent from the sono-Fenton reactor has a lower toxicity than sulfacetamide antibacterial.

Keywords: Sonocatalytic; Sulfacetamide; Zero valent iron nanoparticle; Kinetics; Toxicity test

1. Introduction

Pharmaceuticals consist a large family of human and veterinary medicines, and agricultural products, which have been consumed for many decades [1]. The presence of this compounds in aquatic environment has received increasing attention as emerging contaminates [2]. Antibiotics are a wide range of pharmaceutical compounds, because, due to their persistent nature, they are not treatable in the biological step of sewage treatment plant and accumulate in aquatic environments [2,3].

The related studies have found that low concentration of antibiotics in µg/L or even ng/L level is also a huge threat to the environment and human health [4,5]. In recent years, the introduction of these compounds into the environment without any restrictions may cause bacterial resistance and, as a result, they will not be effective in the treatment of several diseases [6,7]. Sulfonamides are synthetic antibiotics, characterized by sulfonyl group connected to an a mine group and easily soluble in water [6,8]. They are bacteriostatic agents prescribed to treat human and animal infections [9]. Sulfonamides are present in the environment for a long time, due to their low biodegradability, found at concentrations ranging from 0.13 to 1.9 µg/L. Sulfacetamide is a sulfonamide drug that widely used against many gram positive organisms and

*Corresponding author.

some gram negative bacilli. They are effective in the treatment of urinary tract infections and eye infections [8,10].

Advanced oxidation processes (AOPs) have demonstrated to be effective for the treatment of nonbiodegradable compounds [11–14]. AOPs are aqueous phase oxidation processes, which supply hydroxyl radical as a powerful oxidant, resulting in the destruction of the target compound. The advanced Fenton process (AFP) is one of the most powerful AOPs to degrade different pollutions in wastewater [15,16]. Recently, the application of nZVI to eliminate pollutants has drawn great attention due to its higher reactivity and large removal capacity [17]. In the AFP process, Fe is converted to Fe^{2+} and the subsequent reactions are as follows [15].

$$Fe^{3+}))) \rightarrow Fe^{2+} \quad (1)$$

$$Fe^{2+} + H_2O_2 \rightarrow Fe^{3+} + OH^- + HO\cdot \quad (2)$$

$$Fe^{3+} + H_2O_2 \rightarrow Fe - O_2H_2^+ + H^+ \quad (3)$$

$$Fe - O_2H_2^+))) \rightarrow Fe^{2+} + HO_2 \quad (4)$$

Combination of sonolysis and Fenton process is an efficient technique for degradation of hazardous organic pollutants [18]. Sonolysis involves the formation, growth, and collapse of bubbles in liquid, lead to high temperatures and motion in liquid bulk which increase the reactivity by nearly a million fold [19]. This condition is followed by producing highly reactive species including OH°, oxidizing the targeted organic compounds [19]. In the presence of ultrasonic irradiation, H_2O_2 decomposes into OH° and accelerates the degradation process [20]. The nZVI particles have the tendency to aggregate in aqueous solution due to the forces present among them, which result low efficiency in the wastewater treatment. Ultrasonic waves split the mass of nZVI nanoparticles into homogeneous suspensions [21]. Nanoscale zero-valent Iron is widely used to remediate organic and inorganic compounds. The large surface-to-volume ratio of nZVI particles can lead to more reactivity than powders of granular iron [22].

The present work evaluates the degradation of sulfacetamide in water by sono-Fenton process, using nZVI as a catalyst. The effect of initial pH, H_2O_2 concentration, nZVI concentration, irradiation time on the degradation efficiency is investigated, and the kinetics of the process is defined. Additionally, LC-MS analysis was performed to determine the compounds of the decomposition process. The toxicity of treated solution was determined using micro toxicity test.

2. Materials and methods

2.1. Reagents

Sulfacetamide was supplied from Sigma-Aldrich (>99.5%). $FeSO_4{\cdot}7H_2O$, H_2O_2 (30%, w/w in water), $NaBH_4$, HPLC grade methanol were purchased from Merck Company (Darmstadt, Germany). All solutions were prepared in doubly distilled water. All the chemicals used in this study were of the purest grade commercially available and were used directly without further purification.

2.2. Preparation of nZVI particles

The nZVI particles were prepared via an aqueous phase reduction method [23]. The reaction can be described by Eq. (5):

$$4Fe^{3+} + 3BH_4^- + 9H_2O \rightarrow 4Fe^0 \downarrow + 3cH_2BO_3^- + 12H^+ + 6H_2 \quad (5)$$

A three-open-neck round bottom flask reactor was used to synthesis nZVI particles. Ultrasonic probe entered the central neck. N_2 gas was introduced from another neck to exhaust oxygen gas and prevent the oxidation of nanoparticles. The ferrous sulfate solution (0.65 M) was introduced into the reactor. Then, 20 ml of sodium borohydride solution (1.05 M) was added drop wise from the third neck to reduce the ferrous ion to nZVI. A dark suspension containing nZVI particles was formed and the solution was exposed to ultrasonic waves for 5 min, after the reaction was completed. nZVI particles were separated from the solution magnetically, purified three times with deionizer water and ethanol then washed with acetone. Finally, they were dried in a vacuum desiccator at ambient temperature for 24 h.

X-Ray analysis of nanoparticles was performed to determine the surface chemistry, before and after reaction. Nanoparticles map was analyzed by scanning electron microscope. Particle size and morphology of nZVI were identified using transmission electron microscope. FTIR spectroscopy was used to specify the functional group of nZVI before and after reaction.

2.3. Experimental procedure

A 100 ml aqueous solution of sulfacetamide with concentration of 50 mg/L was prepared. The degradation of sulfacetamide was performed in a conical flask placed in a FAPAN 400R model ultrasonic device with a frequency of 24 kHz and 400 W power. The pH of the solution was adjusted using H_2SO_4 and NaOH and measured (Behineh SAT-2002). The experiments were carried out under various initial solution pH values (3,5,7,9), NZVI concentrations (1,3,5,7,8 $g{\cdot}L^{-1}$), H_2O_2 concentrations (0.05, 0.1, 0.3, 0.5, 1.1.5, 2 M) and time (5, 15, 30, 45, 60, 75, 90 min). Detection of sulfacetamide was measured at a wavelength of 270 nm by HPLC (JASCO UV-1575/UV-VIS Detector Intelligent) [C18 250 mm × 4 mm i.d]. Samples were analyzed at a flow rate of 1 mL/min and the injection volume was 20 µL, using 33:67 methanol: sodium dihydrogen phosphate as a mobile phase.

2.4. Toxicity measurements

The toxic effects of untreated and treated solutions were evaluated based on the inhibition of bacterial growth of gram-negative bacteria (Escherichia coli ATCC 2592) and gram-positive bacteria (Staphylococcus aureus ATCC 6538). Each tested bacterial strain was seeded on Lactose broth to reach the OD_{600} 0f 0.1. The solution of sulfacetamide at a concentration of 50 mg/L and the treated solu-

tion were separately added to the prepared culture medium and ancubated at 37°C. Antibiotic activity of the samples was observed by measuring absorbance at a wavelength of 600 nm every 2 h for 10 h. Negative control group including bacterial culture in the absence of antibiotic was used for each test. The inhibitory rate of growth was calculated from the following equation.

$$GI\% = \left(1 - \frac{OD600s}{OD600c}\right) \times 100 \quad (6)$$

where OD is the optical density of the sample measured at 600 nm. OD_{600s} is the OD_{600} of sample and OD_{600c} is the OD_{600} of control.

3. Results and discussion

3.1. Characterization of nZVI

3.1.1. XRD

Fig. 1 shows XRD spectrum of nZVI samples before and after reaction. At angle of 44.67°, the curve has the highest peak that according to the standard of ICDD Card#06.0696, it relates to the presence of Fe°. The peaks at 2ɵ of 36.3° (Fe_3O_4) and 62.9° (Fe_2O_3) reveals the oxidation of nZVI before the reaction, due to exposure to air. The same peaks appeared on the reacted nZVI, but decreased, indicating the removal of Fe^{2+}, consequently reducing the amount of Fe° [24]. According to the standard 039–1346, peaks at 30.225°, 57.275°, indicates the presence of Fe_2O_3 [25]. However, the reacted sample contained peaks at angles of 27.1° and 47°, indicating the presence of y-FeOOH as the result of liquidation of nZVI [26].

3.1.2. SEM

SEM analysis of freshly synthesized nZVI showed a chain-like structure, which is the result of the magnetic interaction between small particles (Fig. 2). SEM image illustrates the spherical and homogeneous morphology of the particles. After using nZVI as a catalyst in heterogeneous sonofenton process, the chain structure was reduced into a large branched structure consisting iron oxide [27]. It is obvious that ultrasonic waves changed the morphology of nZVI to dendritic structure [28]. Also, the compounds, generated through iron oxidation, such as oxide and hydroxide are in the form of needle crystals [26].

3.1.3. TEM

TEM images illustrate that synthesized nanoparticles have core-shell structure and a distinct boundary between the core and the shell (Fig. 3) [29]. The core contains metallic iron and the outer layer contains iron oxide and hydroxides [28]. TEM images indicates the spherical, amorphous and accumulated structure of nZVI. Nanoparticles are visible in the form of irregular clusters [30].

3.1.4. FTIR

The FTIR spectrum was used to identify the involved functional groups in the fresh nZVI and after its oxidation. Fig. 4 refers to FTIR spectra. Peaks in the range of ~3400 cm^{-1} and ~1640 cm^{-1}, respectively, corresponds to O–H stretching vibration group and O–H binding vibration group, which indicates the physisorbed water molecules on the surface of the nanoparticles [31]. The adsorption spectrum of 2920 cm^{-1}, confirms the presence of CH functional group, which disappeared in the FTIR spectra of nZVI after the adsorption reaction. After the oxidation process, the peak at 1391 cm^{-1} appears, which relates to the S=O group. The bands at 670 cm^{-1} and 1047 cm^{-1} correspond to Fe–O stretching functional group [27,29].

3.2. Effect of operational parameters on the degradation of sulfacetamide

3.2.1. Effect of pH

The results of the effect of pH on sulfacetamide removal are illustrated in Fig. 5. The pH is an important controlling parameter that effects Fenton-like process. The results

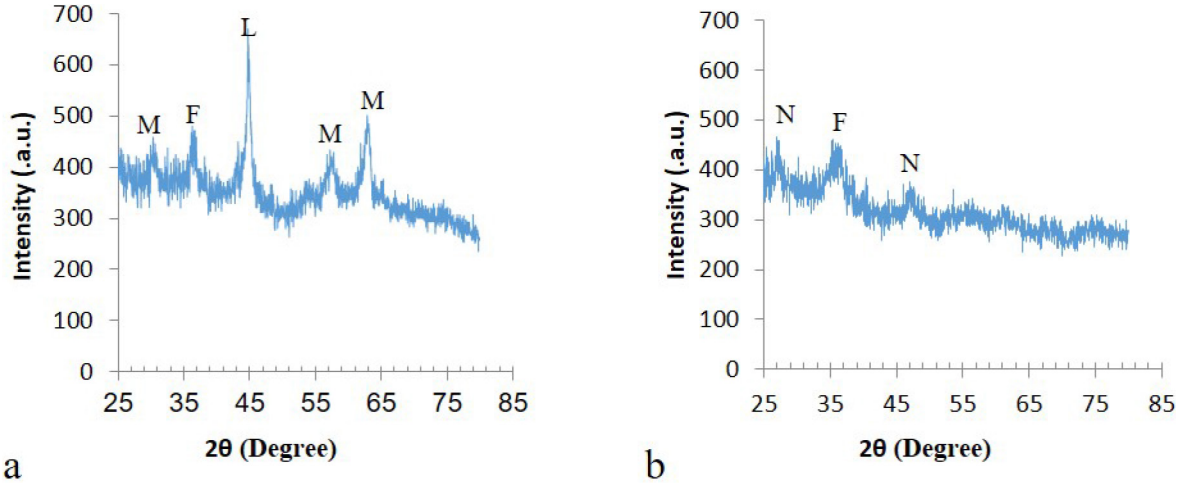

Fig. 1. XRD analysis of fresh nZVI (a), reacted nZVI (b). Peaks refer to Fe_2O_3 (M), Fe_3O_4 (F), Fe^0 (L) and y-FeOOH (N).

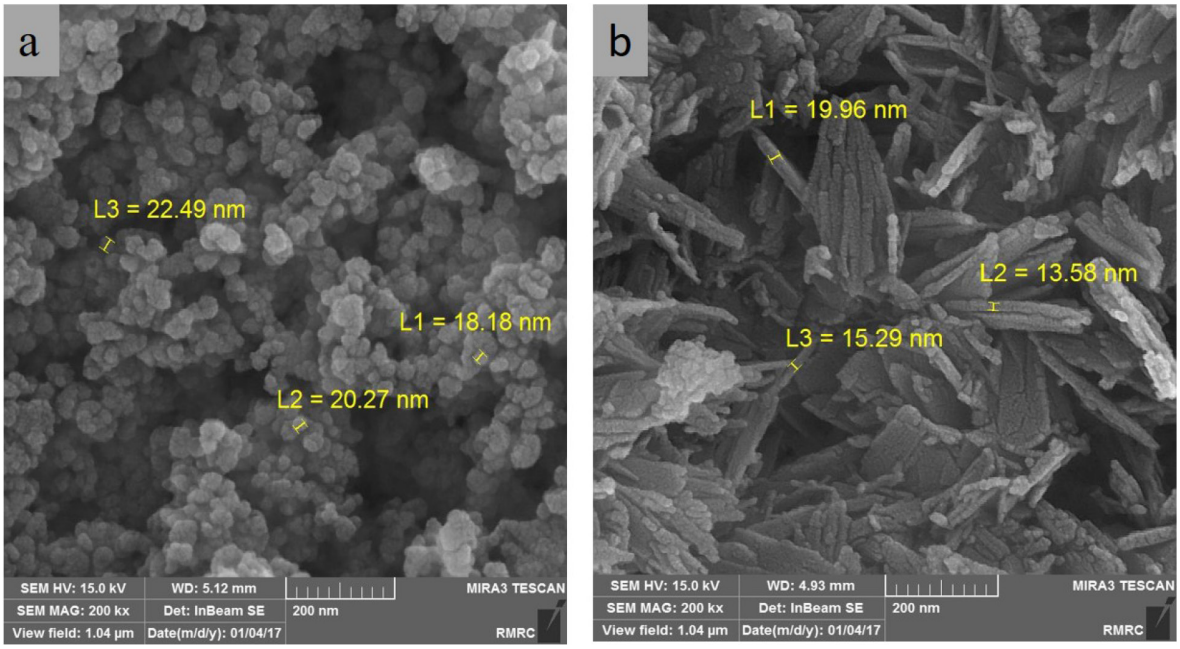

Fig. 2. SEM images of nZVI before (a) and after (b) reaction.

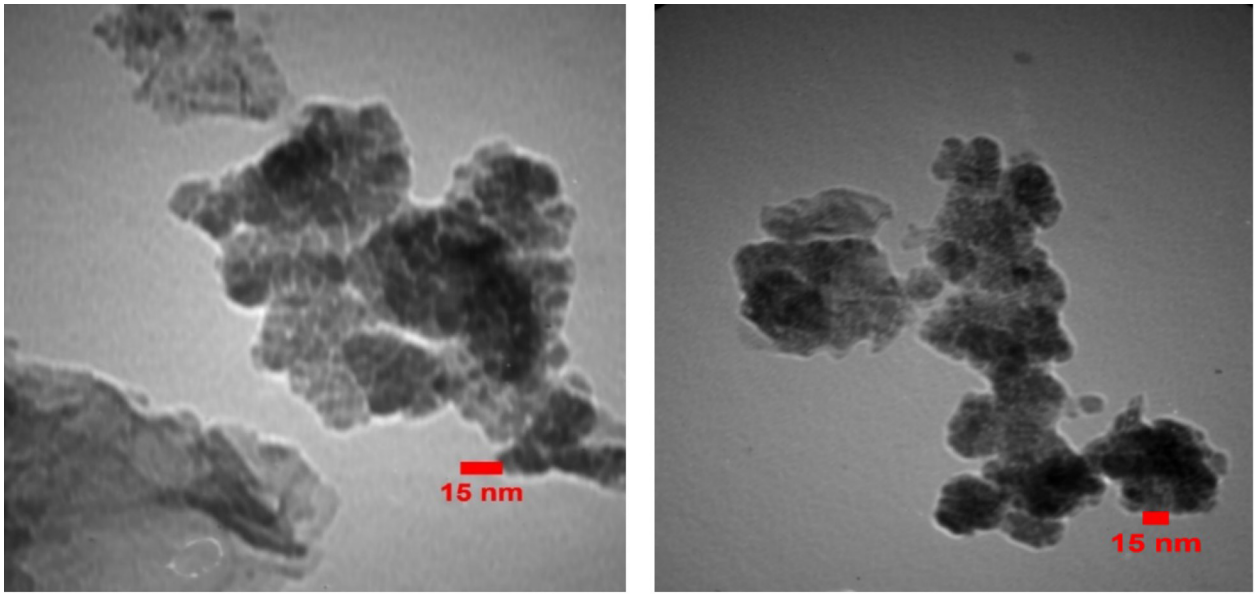

Fig. 3. TEM images of synthesized nZVI.

showed that degradation efficiency decreased with the increase of pH. The highest efficiency of sulfacetamide removal was achieved at pH of 3. This finding is consistent with the result of Zhang et al. [32] in norfloxacin removal using coupled synthesized nZVI with H_2O_2 system. During ultrasonic irradiation and acidic condition, the concentration of Fe^{2+} and OH° radical increases [Eqs.(2) and (7)] [33].

$$Fe^{\circ} + 2H+ \rightarrow Fe^{2+} + H_2 \quad (7)$$

The appropriate pH range for Fenton' s oxidation is between 2 to 4. At pH values of <2, the degradation efficiency decreases due to the formation of iron complex species and formation of oxonium ion $[H_3O_2]^+$. With pH values more than 4, the formation of Ferric-hydroxo complexes inhibits the production of hydroxyl radical therefore, free iron decreases in solution. As a consequence, Fe^{2+} will not be regenerated. Generally, with pH values increased the oxidation potential of hydroxyl radical decreases.

3.2.2. Effect of nZVI dosage

According to Fig. 6, with increasing initial concentration of nZVI from 1 to 8 g/L, the removal efficiency increases

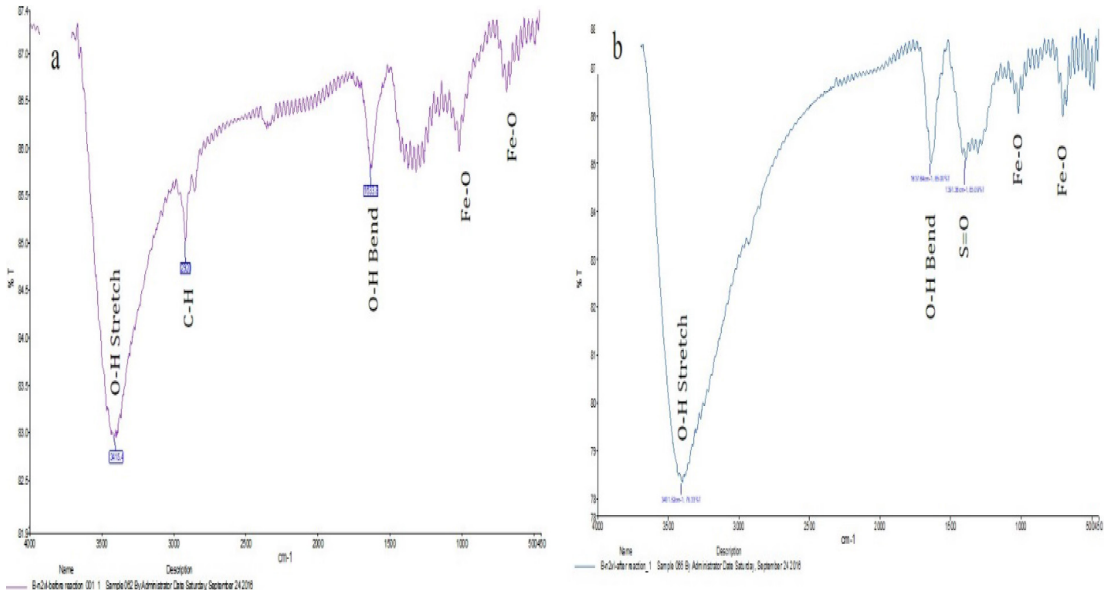

Fig. 4. FTIR spectrum of nZVI before (a) and after (b) reaction.

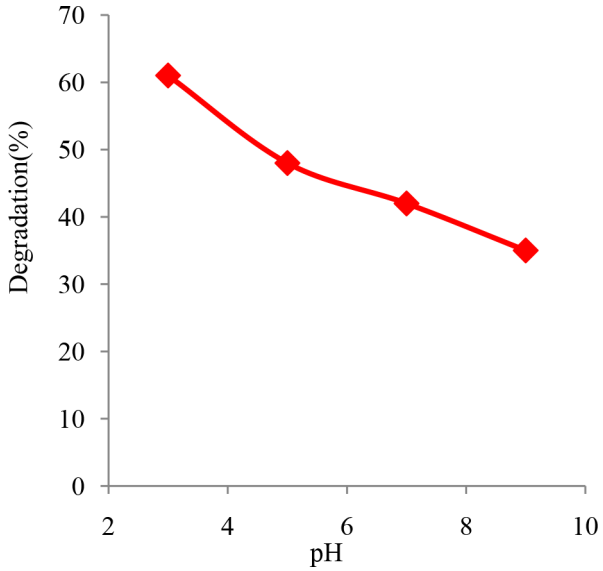

Fig. 5. The effect of pH on the efficiency of sulfacetamide removal (H_2O_2 =0.5 M, nZVI = 1 g/L, t = 30 min).

from 53% to 80%. Which is due to the fact that the increase in active sites, led to more H_2O_2 decomposition and hence producing more OH° radical. By increasing the amount of nZVI from 5 to 8 g/L, the degradation rate increased by 5%, which is almost constant. Therefore 5 g/L considered as the most convenient dose of nZVI. This might be due to the agglomeration of nZVI, resulting the scavenging of hydroxyl radicals through reaction [Eq. (8)] [34].

$$Fe^{2+} + OH^{\circ} \rightarrow Fe^{3+} + OH^{-} \quad (8)$$

This corresponds with a previous research including a study of chlorpheniramine removal using nZVI by Wang et al. [35].

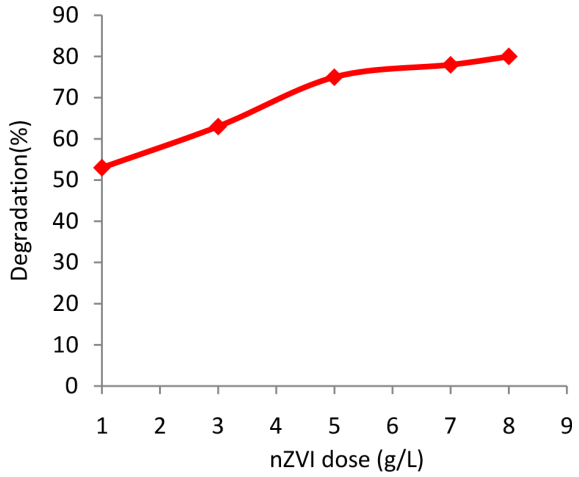

Fig. 6. The effect of nZVI dose on sulfacetamide removal efficiency (pH = 3, H_2O_2 = 0.5 M, t = 30 min).

3.2.3. Effect of H_2O_2 concentration

Fig. 7 shows the effect of H_2O_2 concentration on the oxidative degradation of sulfacetamide. The results illustrate that by an increase in H_2O_2 concentration from 0.05 to 2 M, the degradation efficiency first increased and then decreased, therefore the maximum degradation efficiency was observed at 1 M. This is owning to the formation of more OH° radicals, with the increase of H_2O_2 concentration [35]. However at H_2O_2 concentration >1 M, the degradation efficiency decreased, that might be attributed to the scavenging effect of hydroxyl radicals, which consume OH° radical. Other generated radicals such as HO°_2 are less reactive compared to OH° (Eq.9).

$$OH^{\circ} + H_2O_2 \rightarrow HO^{\circ}_2 + H_2O \quad (9)$$

The results are consistent with the study by Deng et al. [36] in sulfamethazine removal using nZVI/biochar composite.

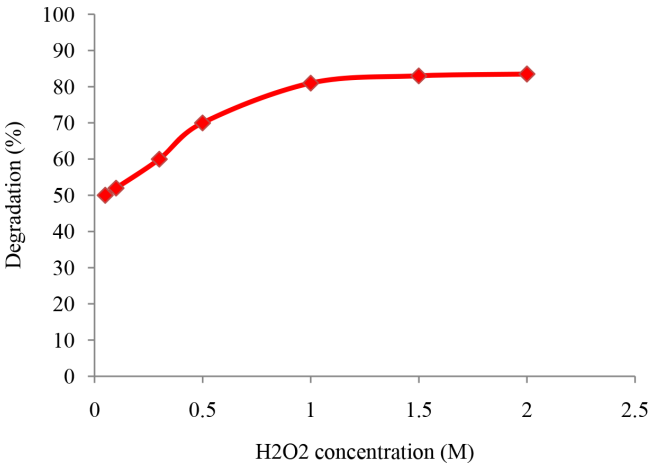

Fig. 7. The effect of H_2O_2 concentration on sulfacetamide removal efficiency (pH = 3, nZVI = 5 g/L, t = 30 min).

3.2.4. Effect of contact time

The effect of contact time on the removal efficiency of sulfacetamide is presented in Fig. 8. As can be seen, by increasing the contact time, the removal efficiency was increased and the maximum degradation efficiency was found to be at 60 min with the passing of time, due to more hydroxyl radical production, degradation efficiency increased. However, by increasing contact time from 60 to 90 min, degradation efficiency is constant. At this stage, the reaction between Fe^{3+} and H_2O_2 results in $HO°_2$ and weaker radical production that decreases the degradation efficiency. On the other hand, remaining empty sites were filled by sulfacetamide [37].

3.3. COD removal

The results of COD reduction in optimal condition are shown in Fig. 9. COD removal (27%) was less than antibiotic removal (91%). It might be attributed to that sulfacetamide has not been completely degraded and might be converted to other organic compounds. Also, the efficiency of enough hydrogen peroxide prevents the oxidation of all organic

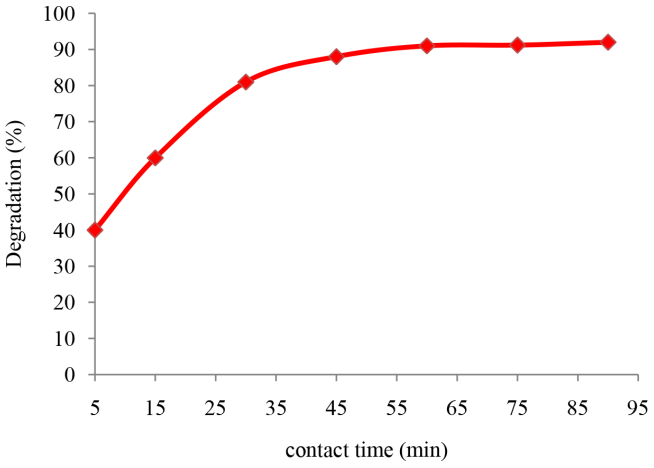

Fig. 8. The effect of time on sulfacetamide removal efficiency (pH = 3, nZVI = 5 g/L, H_2O_2 = 1 M).

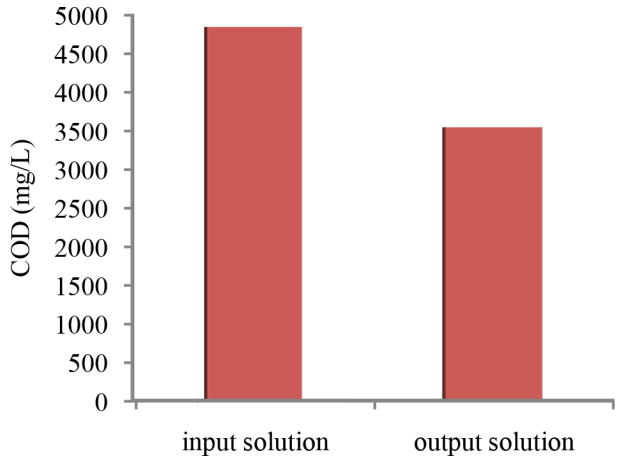

Fig. 9. COD level before and after sono-Fenton process.

compounds. The results correspond with the study of Cui et al. including berberine removal by Fenton oxidation [4].

3.4. Analysis of the synergy in sono-Fenton process

The removal efficiency of individual processes (H_2O_2, nZVI, US) on oxidative degradation, was investigated in optimal condition (pH = 3, nZVI = 5 g/L, H_2O_2 = 1 M, t = 60 min) (Fig. 10). The dominant mechanism was chemical oxidation to produce hydroxyl radical [38]. As can be observed in Fig. 10, when ultrasonic waves were used alone, the degradation efficiency decreased for 79%. This is due the asymmetric distribution of cavitation bubbles therefore, temporal production of OH°. The combination of ultrasonic radiation with Fe° generates more OH°, than ultrasonic waves alone. In the study of Wei et al., the removal of K-2BP by the US-Fe process resulted in 90.5% degradation efficiency after 60 min while under the same condition, only 38.3% and 17% of K-2BP decreased by Fe° and ultrasonic waves, respectively [39]. According to Fig. 10, in the nZVI system, the removal efficiency was 53% less than sonofenton process. The limited activity in nZVI system is due to the magnetic attraction between the nZVI nanoparticles. The magnetic properties of nZVI nanoparticles which make them to agglomerate and as a result the

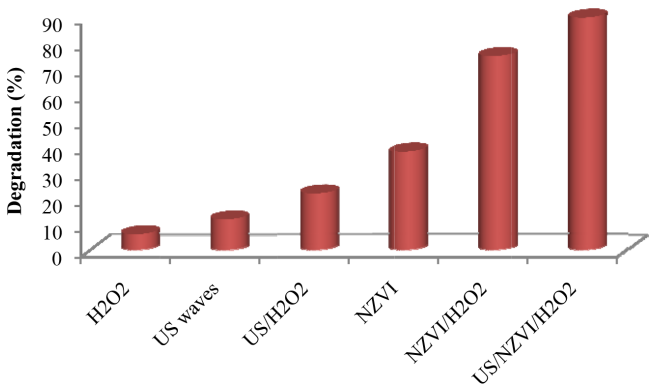

Fig. 10. Removal efficiency of individual processes in optimal condition.

surface area decreases [40,41]. The cavitation phenomenon caused by ultrasonic waves diffuses aggregated nZVIs so more surface area is available for the catalyst [42]. Shrazi et al. demonstrated that the degradation efficiency by using nZVI alone and changing its concentration from 0.3 to 5 g/L have not increased and the carbamazepine removal was less than 5% [43]. The degradation efficiency by H_2O_2 in optimal condition was 6% that showed a significant reduction compared to sonofenton process, indicating the low rate of hydroxyl radical production via H_2O_2. Indeed, nZVI acts as an amplifier agent in heterogeneous Fenton-like process and increases the surface area. The degradation efficiency of amoxicillin in H_2O_2 and nZVI/H_2O_2 system, were 0.2% and 86.5% respectively, which confirms the results of this study [27]. But it was observed that there was an increasing trend in degradation by combining these factors together. So, the highest amount of removal was seen in the heterogeneous Sono Fenton oxidation process, at around 90%.

3.5. Kinetic study

In the present study, two kinetic models were used, including pseudo-first-order and pseudo-second-order models. The liner form of pseudo-first-order kinetic is:

Pseudo-first-order equation:

$$In\frac{C_t}{C_o} = -K_1 t \tag{10}$$

where C_t is the residual concentration of sulfacetamide at time t (mg/L), C_0 is the initial concentration of sulfacetamide (mg/L) and K_1 is the rate constant of pseudo-first-order mode (min^{-1}) and t is the time (min).

The liner form of second-order kinetic is:

Pseudo-second-order equation: $$\frac{1}{C_t} = K_2 t + \frac{1}{C_0} \tag{11}$$

where K_2 is the rate constant of pseudo-second-order model ($mg \cdot g^{-1} \cdot min^{-1}$).

The results showed that the kinetic of sulfacetamide degradation by sonofenton process as shown in Fig. 11 follow pseudo-second-order model (R^2 = 0.9936). Zhang et al. [32] and Shemer et al. [44] introduced the removal of norfloxacin and metronidazole, respectively, using Fenton process based on pseudo-second-order kinetic model.

3.6. Microtoxicity study

AOP degradation process can produce intermediates more toxic than primary compound [45]. The results showed that the growth inhibition percentage (GI%) of treated solution decreased (Table 1). Elimination of interfering effect of H_2O_2 performed by increasing pH above 10 and H_2O_2 decomposition into water and oxygen [46]. Photo catalytic degradation of sulfacetamide, sulfathiazole, sulfamethoxazole and sulfadiazine indicated that the toxicity level (EC50) increased in contrast: sulfacetamide, sulfathiazole, sulfamethoxazole, sulfadiazine and the intermediate compounds were less toxic than parent compounds [9]. Trovo et al. observed a 65% reduction in the toxicity of sulfamethoxazole with an increase in H_2O_2 from 10 mg/L to 20 mg/L [3].

3.7. LC/MS analysis

LC/MS analysis is commonly used to determine the combinations derived from antibiotic degradation. The analysis of the results is based on the value (m/z). The LC/MS analysis results are shown in Fig. 12. Table 2 shows the compounds of sulfacetamide decomposition. As the results showed, the destruction of the antibiotic structure and

Table 1
Growth inhibition percentage (GI%) of treated and untreated solution

Microorganism	Sulfacetamide	
	Untreated	Treated
E. coli	75 ± 0.3	45 ± 0.2
S.aureus	73 ± 0.2	40

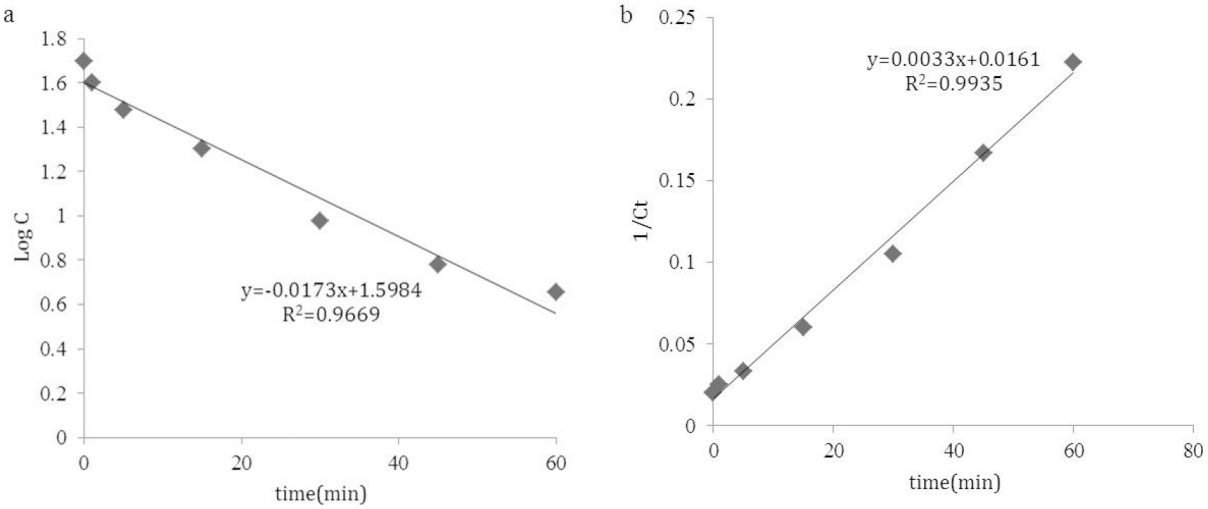

Fig. 11. Pseudo-first-order (a) and pseudo-second-order (b) kinetic curve for sulfacetamide removal.

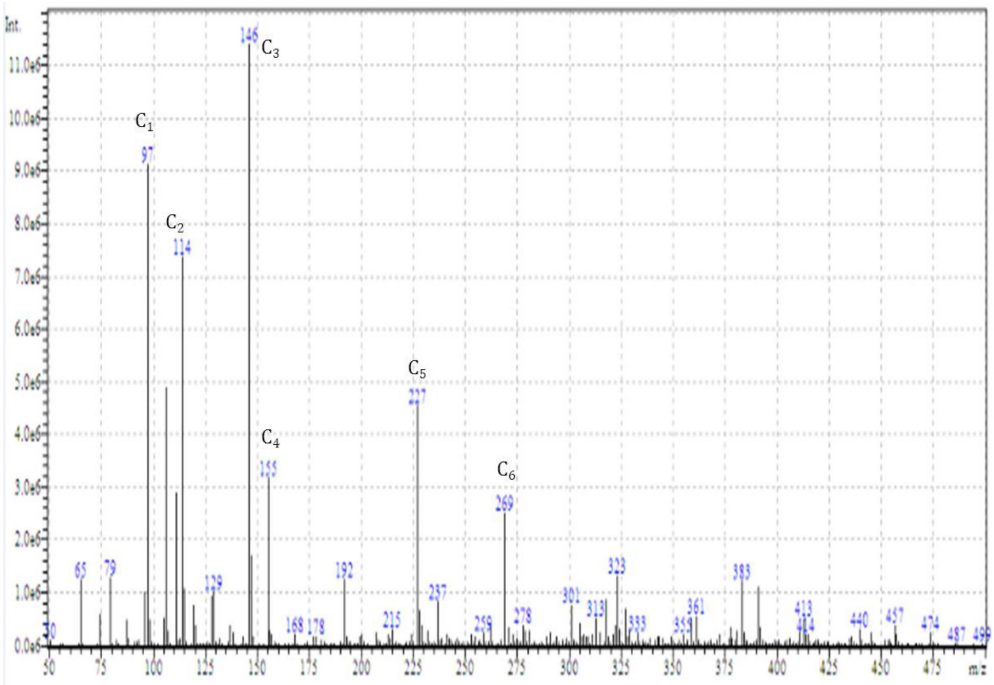

Fig. 12. LC/MS analysis.

Table 2
LC/MS analysis results

Compound name	Molecular formula	*m/z*	Chemical compound
C_1	97	$C_4H_5N_2O$	2-nitrosobutanenitrile
C_2	114	$C_4H_6N_2O_2$	piperazine-2,5-dione
C_3	146	$C_6H_{14}N_2O_2$	Alpha-methylornithine
C_4	155	$C_6H_5NO_2S$	3-Mercaptopicolinic acid
C_5	227	$C_{11}H_{17}NO_2S$	N-Butyl-p-toluenesulfonamide
C_6	269	$C_{10}H_{11}N_3O_4S$	1-(2-methoxyethyl)-7-methylsulfanylpyrimido[4,5-d][1,3] oxazine-2,4-dione

the breakdown of the bond between the aminosulfon and methyl led to form C_1 structure with $m/z = 97$. The proposed molecular structure of this compound is $C_4H_5N_2O$ [47]. The existence of C_2 ion with $m/z = 114$ represents the destruction of the structure of sulfacetamide by radical OH° which is observed in most decomposition compounds [3]. The peak generated on the chromatogram at $m/z = 269$ shows the hydroxylation of sulfacetamide (M + H) with the molecular formula of $C_{10}H_{11}N_3O_4S$ [48]. The hydroxyl radical attacked the aniline ring in the antibiotic structure and replaced the amine group. The result of the above process is the formation of $C_6H_5NO_2S$ with $m/z = 155$ [3]. The chemical composition of C_3 with $m/z = 146$ is the result of the hydroxyl radical bond to the structure of the benzene ring [47].

4. Conclusion

In this study, nZVI nanoparticles were used as a catalyst in sono–Fenton like process to degrade sulfacetamide. The optimal conditions for degradation process were pH = 3, 5 g/L nZVI, 1 M H_2O_2 and 60 min reaction time. In this condition, sulfacetamide and COD removal were 91% and 27% respectively. The growth inhibition percentage (GI %) of treated solution decreased significantly. Thus, sonofenton process can be used as a suitable method for sulfacetamide removal.

Acknowledgment

The authors are acknowledged for the financial and instrumental support of the Ardabil University of Medical Sciences.

References

[1] M. Pérez-Moya, M. Graells, G. Castells, J. Amigó, E. Ortega, G. Buhigas, L.M. Pérez, H.D. Mansilla, Characterization of the degradation performance of the sulfamethazine antibiotic by photo-Fenton process, Water Res., 44 (2010) 2533–2540.

[2] J. Wu, H. Zhang, N. Oturan, Y. Wang, L. Chen, M.A. Oturan, Application of response surface methodology to the removal of the antibiotic tetracycline by electrochemical process using carbon-felt cathode and DSA (Ti/RuO_2–IrO_2) anode, Chemosphere, 87 (2012) 614–620.
[3] A.G. Trovó, R.F. Nogueira, A. Agüera, A.R. Fernandez-Alba, C. Sirtori, S. Malato, Degradation of sulfamethoxazole in water by solar photo-Fenton. Chemical and toxicological evaluation, Water Res., 43 (2009) 3922–3931.
[4] X. Cui, P. Zeng, G. Qiu, Y. Liu, Y. Song, X. Xie, L. Han, Pilot-scale treatment of pharmaceutical berberine wastewater by Fenton oxidation, Environ. Earth Sci., 73 (2015) 4967–4977.
[5] W. Xiong, Z. Zeng, X. Li, G. Zeng, R. Xiao, Z. Yang, Y. Zhou, C. Zhang, M. Cheng, L. Hu, Multi-walled carbon nanotube/amino-functionalized MIL-53 (Fe) composites: remarkable adsorptive removal of antibiotics from aqueous solutions, Chemosphere, 210 (2018) 1061–1069.
[6] V. Homem, L. Santos, Degradation and removal methods of antibiotics from aqueous matrices – a review, J. Environ. Manage., 92 (2011) 2304–2347.
[7] Y. Yang, Z. Zeng, C. Zhang, D. Huang, G. Zeng, R. Xiao, C. Lai, C. Zhou, H. Guo, W. Xue, Construction of iodine vacancy-rich BiOI/Ag@ AgI Z-scheme heterojunction photo catalysts for visible-light-driven tetracycline degradation: transformation pathways and mechanism insight, Chem. Eng. J., 349 (2018) 808–821.
[8] A. Dirany, I. Sirés, N. Oturan, M.A. Oturan, Electrochemical abatement of the antibiotic sulfamethoxazole from water, Chemosphere, 81 (2010) 594–602.
[9] W. Baran, J. Sochacka, W. Wardas, Toxicity and biodegradability of sulfonamides and products of their photo catalytic degradation in aqueous solutions, Chemosphere, 65 (2006) 1295–1299.
[10] C. Zhou, P. Xu, C. Lai, C. Zhang, G. Zeng, D. Huang, M. Cheng, L. Hu, W. Xiong, X. Wen, Rational design of graphic carbon nitride copolymers by molecular doping for visible-light-driven degradation of aqueous sulfamethazine and hydrogen evolution, Chem. Eng. J., 359 (2019) 186–196.
[11] T. Methatham, M.-C. Lu, C. Ratanatamskul, Removal of 2, 4-dichlorophenol as herbicide's by-product by Fenton's reagent combined with an electrochemical system, Desal. Water Treat., 32 (2011) 42–48.
[12] H. Yi, M. Yan, D. Huang, G. Zeng, C. Lai, M. Li, X. Huo, L. Qin, S. Liu, X. Liu, Synergistic effect of artificial enzyme and 2D nano-structured Bi_2WO_6 for eco-friendly and efficient biomimetic photo catalysis, Appl. Catal., B., 250 (2019) 52–62.
[13] Y. Yang, C. Zhang, C. Lai, G. Zeng, D. Huang, M. Cheng, J. Wang, F. Chen, C. Zhou, W. Xiong, BiOX (X=Cl, Br, I) photo catalytic nanomaterials: applications for fuels and environmental management, Adv. Colloid Interfac., 254 (2018) 76–93.
[14] C. Zhang, W. Wang, A. Duan, G. Zeng, D. Huang, C. Lai, X. Tan, M. Cheng, R. Wang, C. Zhou, Adsorption behavior of engineered carbons and carbon nanomaterials for metal endocrine disruptors: Experiments and theoretical calculation, Chemosphere, 222 (2019) 184–194.
[15] F. Yehia, G. Eshaq, A. Rabie, A. Mady, A. ElMetwally, Phenol degradation by advanced Fenton process in combination with ultrasonic irradiation, Egyptian J. Petrol., 24 (2015) 13–18.
[16] Y. Yang, C. Zhang, D. Huang, G. Zeng, J. Huang, C. Lai, C. Zhou, W. Wang, H. Guo, W. Xue, Boron nitride quantum dots decorated ultra thin porous g-C_3N_4: intensified exciton dissociation and charge transfer for promoting visible-light-driven molecular oxygen activation, Appl. Catal., B., 245 (2019) 87–99.
[17] F. Fu, D.D. Dionysiou, H. Liu, The use of zero-valent iron for groundwater remediation and wastewater treatment: a review, J. Hazard. Mater., 267 (2014) 194–205.
[18] M.A.N. Khan, M. Siddique, F. Wahid, R. Khan, Removal of reactive blue 19 dye by sono, photo and sono photo catalytic oxidation using visible light, Ultrason. Sonochem., 26 (2015) 370–377.
[19] R. Bhavani, A. Sivasamy, Sonocatalytic degradation of malachite green oxalate by a semiconductor metal oxide nanocatalyst, Ecotox. Environ. Safe., 134 (2016) 403–411.
[20] Y.L. Pang, A.Z. Abdullah, S. Bhatia, Review on sonochemical methods in the presence of catalysts and chemical additives for treatment of organic pollutants in wastewater, Desalination, 277 (2011) 1–14.
[21] X. Zhou, B. Lv, Z. Zhou, W. Li, G. Jing, Evaluation of highly active nanoscale zero-valent iron coupled with ultrasound for chromium (VI) removal, Chem. Eng. J., 281 (2015) 155–163.
[22] N.C. Mueller, B. Nowack, Nanoparticles for remediation: solving big problems with little particles, Elements, 6 (2010) 395–400.
[23] Y. Liu, H. Choi, D. Dionysiou, G.V. Lowry, Trichloroethene hydrodechlorination in water by highly disordered monometallic nanoiron, Chem. Mater., 17 (2005) 5315–5322.
[24] R. Li, X. Jin, M. Megharaj, R. Naidu, Z. Chen, Heterogeneous Fenton oxidation of 2, 4-dichlorophenol using iron-based nanoparticles and persulfate system, Chem. Eng. J., 264 (2015) 587–594.
[25] D. Mohan, S. Kumar, A. Srivastava, Fluoride removal from ground water using magnetic and nonmagnetic corn stover biochars, Ecol. Eng., 73 (2014) 798–808.
[26] A. Liu, J. Liu, B. Pan, W.-x. Zhang, Formation of lepidocrocite (γ–FeOOH) from oxidation of nanoscale zero-valent iron (nZVI) in oxygenated water, Rsc Adv., 4 (2014) 57377–57382.
[27] S. Zha, Y. Cheng, Y. Gao, Z. Chen, M. Megharaj, R. Naidu, Nanoscale zero-valent iron as a catalyst for heterogeneous Fenton oxidation of amoxicillin, Chem. Eng. J., 255 (2014) 141–148.
[28] M.R. Jamei, M.R. Khosravi, B. Anvaripour, A novel ultrasound assisted method in synthesis of NZVI particles, Ultrason. Sonochem., 21 (2014) 226–233.
[29] A. Liu, J. Liu, W.-x. Zhang, Transformation and composition evolution of nanoscale zero valent iron (nZVI) synthesized by borohydride reduction in static water, Chemosphere, 119 (2015) 1068–1074.
[30] T. Shahwan, S.A. Sirriah, M. Nairat, E. Boyacı, A.E. Eroğlu, T.B. Scott, K.R. Hallam, Green synthesis of iron nanoparticles and their application as a Fenton-like catalyst for the degradation of aqueous cationic and anionic dyes, Chem. Eng. J., 172 (2011) 258–266.
[31] Z. Wen, Y. Zhang, C. Dai, Removal of phosphate from aqueous solution using nanoscale zerovalent iron (nZVI), Colloids Surf. A., 457 (2014) 433–440.
[32] W. Zhang, H. Gao, J. He, P. Yang, D. Wang, T. Ma, H. Xia, X. Xu, Removal of norfloxacin using coupled synthesized nanoscale zero-valent iron (nZVI) with H_2O_2 system: Optimization of operating conditions and degradation pathway, Sep. Purif. Technol., 172 (2017) 158–167.
[33] H. Zhou, Y. Shen, P. Lv, J. Wang, P. Li, Degradation pathway and kinetics of 1-alkyl-3-methylimidazolium bromides oxidation in an ultrasonic nanoscale zero-valent iron/hydrogen peroxide system, J. Hazard. Mater., 284 (2015) 241–252.
[34] A. Babuponnusami, K. Muthukumar, Removal of phenol by heterogenous photo electro Fenton-like process using nanozero valent iron, Sep. Purif. Technol., 98 (2012) 130–135.
[35] L. Wang, J. Yang, Y. Li, J. Lv, J. Zou, Removal of chlorpheniramine in a nanoscale zero-valent iron induced heterogeneous Fenton system: Influencing factors and degradation intermediates, Chem. Eng. J., 284 (2016) 1058–1067.
[36] J. Deng, H. Dong, C. Zhang, Z. Jiang, Y. Cheng, K. Hou, L. Zhang, C. Fan, Nanoscale zero-valent iron/biochar composite as an activator for Fenton-like removal of sulfamethazine, Sep. Purif. Technol., 202 (2018) 130–137.
[37] C. Özdemir, M.K. Öden, S. Şahinkaya, D. Güçlü, The sonochemical decolorisation of textile azo dye CI Reactive Orange 127, Color Technol., 127 (2011) 268–273.
[38] Y. Pan, M. Zhou, J. Cai, X. Li, W. Wang, B. Li, X. Sheng, Z. Tang, Significant enhancement in treatment of salty wastewater by pre–magnetization Fe^0/H_2O_2 process, Chem. Eng. J., 339 (2018) 411–423.
[39] Y. Wei, X. Wang, W. Guo, J. Wang, Mechanistic study of the degradation of azo dye reactive brilliant red K-2BP by ultra sound radiation and zero-valent iron, Environ. Eng. Sci., 29 (2012) 399–405.

[40] Z. Li, L. Wang, J. Meng, X. Liu, J. Xu, F. Wang, P. Brookes, Zeolite-supported nanoscale zero-valent iron: new findings on simultaneous adsorption of Cd (II), Pb (II), and As (III) in aqueous solution and soil, J. Hazard. Mater., 344 (2018) 1–11.
[41] Y.-b. Hu, X.-y. Li, Influence of a thin aluminum hydroxide coating layer on the suspension stability and reductive reactivity of nanoscale zero-valent iron, Appl. Catal. B., 226 (2018) 554–564.
[42] N. Jaafarzadeh, A. Takdastan, S. Jorfi, F. Ghanbari, M. Ahmadi, G. Barzegar, The performance study on ultrasonic/Fe_3O_4/H_2O_2 for degradation of azo dye and real textile wastewater treatment, J. Mol. Liq., 256 (2018) 462–470.
[43] E. Shirazi, A. Torabian, G. Nabi-Bidhendi, Carbamazepine Removal from groundwater: Effectiveness of the TiO_2/UV, nanoparticulate zero-valent fron, and fenton (NZVI/H_2O_2) processes, CLEAN–Soil, Air, Water, 41 (2013) 1062–1072.
[44] H. Shemer, Y.K. Kunukcu, K.G. Linden, Degradation of the pharmaceutical metronidazole via UV, Fenton and photo-Fenton processes, Chemosphere, 63 (2006) 269–276.
[45] R.B. Phillips, R.R. James, M.L. Magnuson, Electrolyte selection and microbial toxicity for electrochemical oxidative water treatment using a boron-doped diamond anode to support site specific contamination incident response, Chemosphere, 197 (2018) 135–141.
[46] I. Talinli, G. Anderson, Interference of hydrogen peroxide on the standard COD test, Water Res., 26 (1992) 107–110.
[47] A.G. Trovó, R.F. Nogueira, A. Agüera, C. Sirtori, A.R. Fernández-Alba, Photo degradation of sulfamethoxazole in various aqueous media: persistence, toxicity and photo products assessment, Chemosphere, 77 (2009) 1292–1298.
[48] H. Lin, J. Niu, J. Xu, Y. Li, Y. Pan, Electrochemical mineralization of sulfamethoxazole by Ti/SnO_2-Sb/Ce-PbO_2 anode: kinetics, reaction pathways, and energy cost evolution, Electrochim. Acta, 97 (2013) 167–174.